Current Biology 24, 2968–2974, December 15, 2014 ©2014 Elsevier Ltd All rights reserved http://dx.doi.org/10.1016/j.cub.2014.11.012

Report

Converging Axons Collectively Initiate and Maintain Synaptic Selectivity in a Constantly Remodeling Sensory Organ

Jesús Pujol-Martí,[1,5] Adèle Faucherre,[2,5] Razina Aziz-Bose,[4] Amir Asgharsharghi,[1] Julien Colombelli,[3] Josef G. Trapani,[4] and Hernán López-Schier[1,2,*]

[1]Unit of Sensory Biology & Organogenesis, Helmholtz Zentrum München, Ingolstädter Landstraße 1, 85764 Munich, Germany

[2]Centre for Genomic Regulation, Dr. Aiguader 88, 08003 Barcelona, Spain

[3]Institute for Research in Biomedicine, Baldiri Reixac 10, 08028 Barcelona, Spain

[4]Department of Biology and Neuroscience Program, Amherst College, Amherst, MA 01002-5000, USA

Summary

Sensory receptors are the functional link between the environment and the brain [1–3]. The repair of sensory organs enables animals to continuously detect environmental stimuli [4]. However, receptor cell turnover can affect sensory acuity by changing neural connectivity patterns [5, 6]. In zebrafish, two to four postsynaptic lateralis afferent axons converge into individual peripheral mechanosensory organs called neuromasts, which contain hair cell receptors of opposing planar polarity [7]. Yet, each axon exclusively synapses with hair cells of identical polarity during development and regeneration to transmit unidirectional mechanical signals to the brain [8, 9]. The mechanism that governs this exceptionally accurate and resilient synaptic selectivity remains unknown. We show here that converging axons are mutually dependent for polarity-selective connectivity. If rendered solitary, these axons establish simultaneous functional synapses with hair cells of opposing polarities to transmit bidirectional mechanical signals. Remarkably, nonselectivity by solitary axons can be corrected upon the reintroduction of additional axons. Collectively, our results suggest that lateralis synaptogenesis is intrinsically nonselective and that interaxonal interactions continuously rectify mismatched synapses. This dynamic organization of neural connectivity may represent a general solution to maintain coherent synaptic transmission from sensory organs undergoing frequent variations in the number and spatial distribution of receptor cells.

Results and Discussion

Hearing, balance, and the determination of the direction of water flow in vertebrates are based on vectorial mechanosensation mediated by the conserved planar orientation of epithelial receptors called hair cells [2]. The piscine mechanosensory lateral line comprises a series of organs called neuromasts (NMs), which contain approximately 20 hair cells divided equally into two populations that are plane polarized at 180° relative to one other (Figures 1A and 1B) [7]. Injured hair cells in NMs are constantly replaced by proliferative regeneration. Remarkably, even under the perpetual instability caused by frequent hair cell turnover, lateralis afferent neurons always innervate hair cells of identical planar polarity. Here, we analyze the mechanism that underlies this strict and resilient synaptic selectivity.

For this study, we first generated double-transgenic zebrafish larvae expressing a GFP in hair cell plasma membranes (memEGFP) and an orange fluorescent protein fused to the A domain of Ctbp2/Ribeye-b (Kus-Rib) (Figures 1C and 1D). Ctbp2/Ribeye-b is an essential component of hair cell presynaptic active zones [10, 11]. We verified the active-zone localization of Kus-Rib by immunohistochemistry using a specific antibody to zebrafish Ctbp2/Ribeye (Figure 1E). To visualize sensory-neural contacts in vivo, we sparse labeled afferent neurons by mosaic expression of mCherry under the transcriptional control of the "SILL" enhancer in *Tg[Brn3c:memEGFP;Brn3c:Kus-Rib]* double-transgenic fish (Figure 1F) [12]. We certified putative synapses when postsynaptic axonal termini juxtaposed Kus-Rib puncta in hair cells using a z series of confocal-microscopy images in larvae at 5–7 days postfertilization (dpf) (Figures 1F and 1G; Movie S1 available online). In control NMs with a normal complement of neurons, individually marked axons innervated about one-half of the constituent hair cells (52% ± 6%, N = 8 NMs) (Figures 1H and 1K). Fluorescent labeling of apical stereocilia showed hair cells of both planar polarities (Figure 1G′) and that each axon innervated hair cells of identical orientation (Figures 1G–1H).

We reasoned that this strict sensory-neural connectivity might be instructed by either (1) a chemoaffinity code or (2) correlated hair cell activity. Both of these ideas predict that axons should autonomously discriminate coherent versus incoherent connectivity, i.e., polarity-exclusive versus promiscuous synapses. Under this scenario, therefore, an axon should remain selective irrespectively of the presence of other axons. To test this hypothesis, we generated zebrafish larvae with NMs innervated by just one axon taking advantage of zebrafish lacking Neurogenin-1, which do not develop any lateralis afferent neurons [13, 14]. Then, in Neurogenin-1-deficient *Tg[HGn39D;Brn3c:memEGFP]* doubly-transgenic "host" embryos, we rescued the production of a few lateralis neurons by transplanting cells from wild-type Tg[SILL1] transgenic "donor" embryos (Figures S1A and S1B). Surprisingly, the "solitary" axons innervated a majority of NM hair cells, which must have both planar orientations (84% ± 11%, N = 8 NMs) (Figures 1I and 1K). Hair cells of neurogenin-1-deficient zebrafish remain mechanoreceptive and maintain the expected planar polarity [14]. We confirmed that these receptors were functional by imaging changes in internal calcium concentration during mechanical stimulation. Control and Neurogenin-1-deficient larvae with hair cell expression of the fluorescent calcium indicator GCaMP7a were mounted in low-melting point agarose with the trunk exposed. We then stimulated a NM with a unidirectional water jet and observed robust mechanotransduction in Neurogenin-1-deficient hair cells (Movie S2; Figure S3). Previous work using nonmechanoreceptive TMIE mutant zebrafish and neurite bulging as a proxy for synaptogenesis suggested that evoked activity affects lateralis synaptic selectivity [8]. We directly tested this possibility

[5]Co-first author

*Correspondence: hernan.lopez-schier@helmholtz-muenchen.de

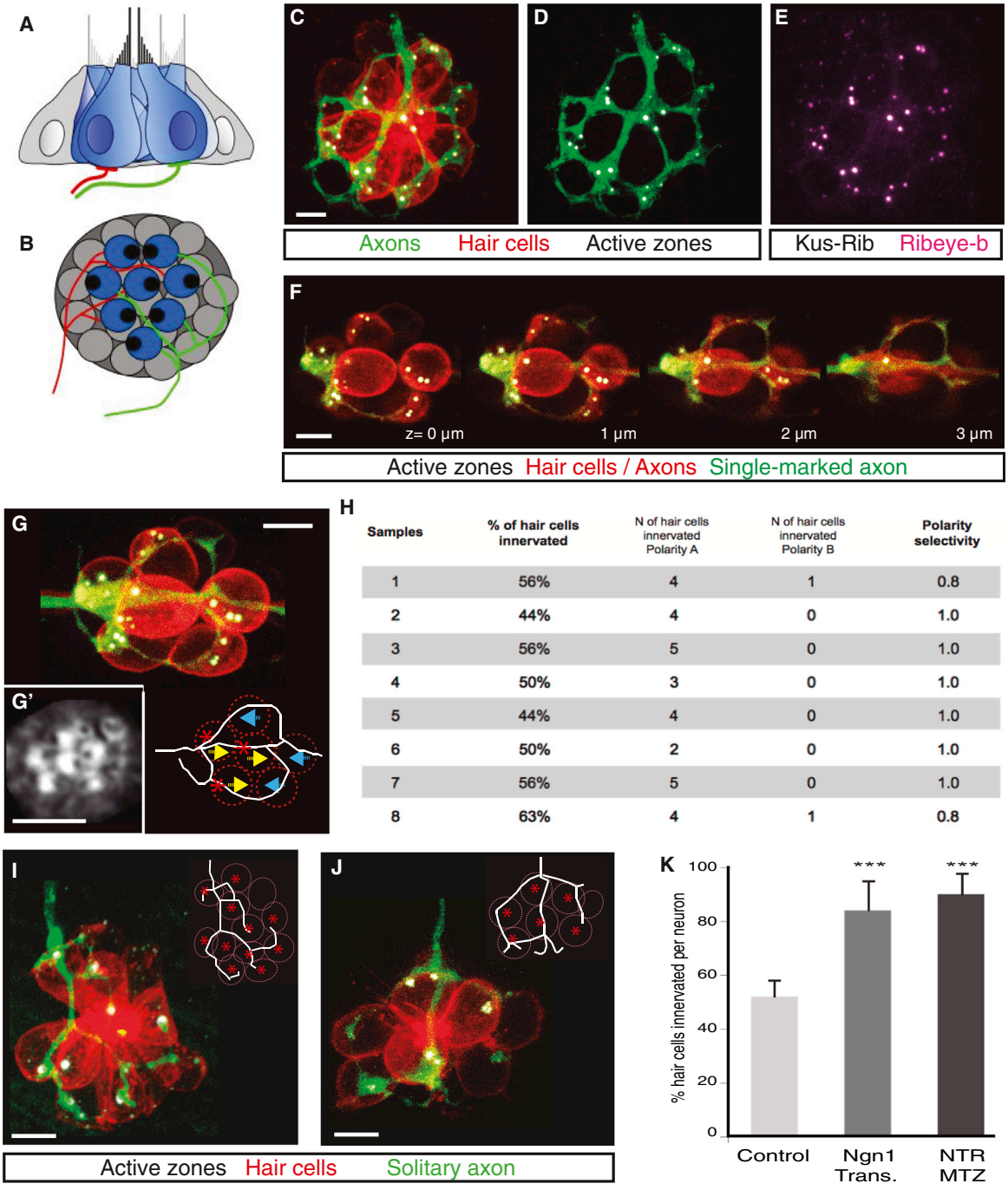

H

Samples	% of hair cells innervated	N of hair cells innervated Polarity A	N of hair cells innervated Polarity B	Polarity selectivity
1	56%	4	1	0.8
2	44%	4	0	1.0
3	56%	5	0	1.0
4	50%	3	0	1.0
5	44%	4	0	1.0
6	50%	2	0	1.0
7	56%	5	0	1.0
8	63%	4	1	0.8

Figure 1. Hair-Cell Innervation by Normal and Solitary Axons

(A and B) Drawings of a control neuromast depicting synaptic selectivity in the lateral line. Each afferent neuron (in green and red) exclusively synapses with hair cells (in blue) of identical planar orientation. Lateral views are shown in (A), and top views are shown in (B).

(C–E) Control neuromast with all afferent axons, hair cells, and presynaptic active zones labeled.

(D) Kus-Rib transgene reveals presynaptic active zones abutting axonal termini.

(E) Colocalization of Kus-Rib transgene and endogenous Ribeye-b (revealed by immunohistochemistry).

(F–G′) Consecutive stacks (F) and maximal projection (G) of single-marked axon in a control neuromast. Actin labeling with fluorescent phalloidin (G′) reveals hair cell planar polarity in (G). Drawing in (G) depicts an axon that innervates 50% of the hair cells (asterisks), all of identical orientation (represented by color-coded arrows).

(H) Quantification of polarity selectivity by individual axons in control neuromasts. Strict selectivity = 1; no selectivity = 0.5. Polarity selectivity was calculated as described in the Supplemental Experimental Procedures.

(I and J) Neuromasts innervated by a solitary axon resulting from ngn1-MO/transplantation (I) and nitroreductase (NTR)/metronidazole (MTZ) (J) strategies. Insets quantify synaptic contacts (asterisks) between the axon termini and the hair cells.

(K) Quantification of hair cell innervation by control and solitary axons. Error bars represent the SD. ***$p < 0.01$ (Student's t test).

Scale bars represent 5 µm.

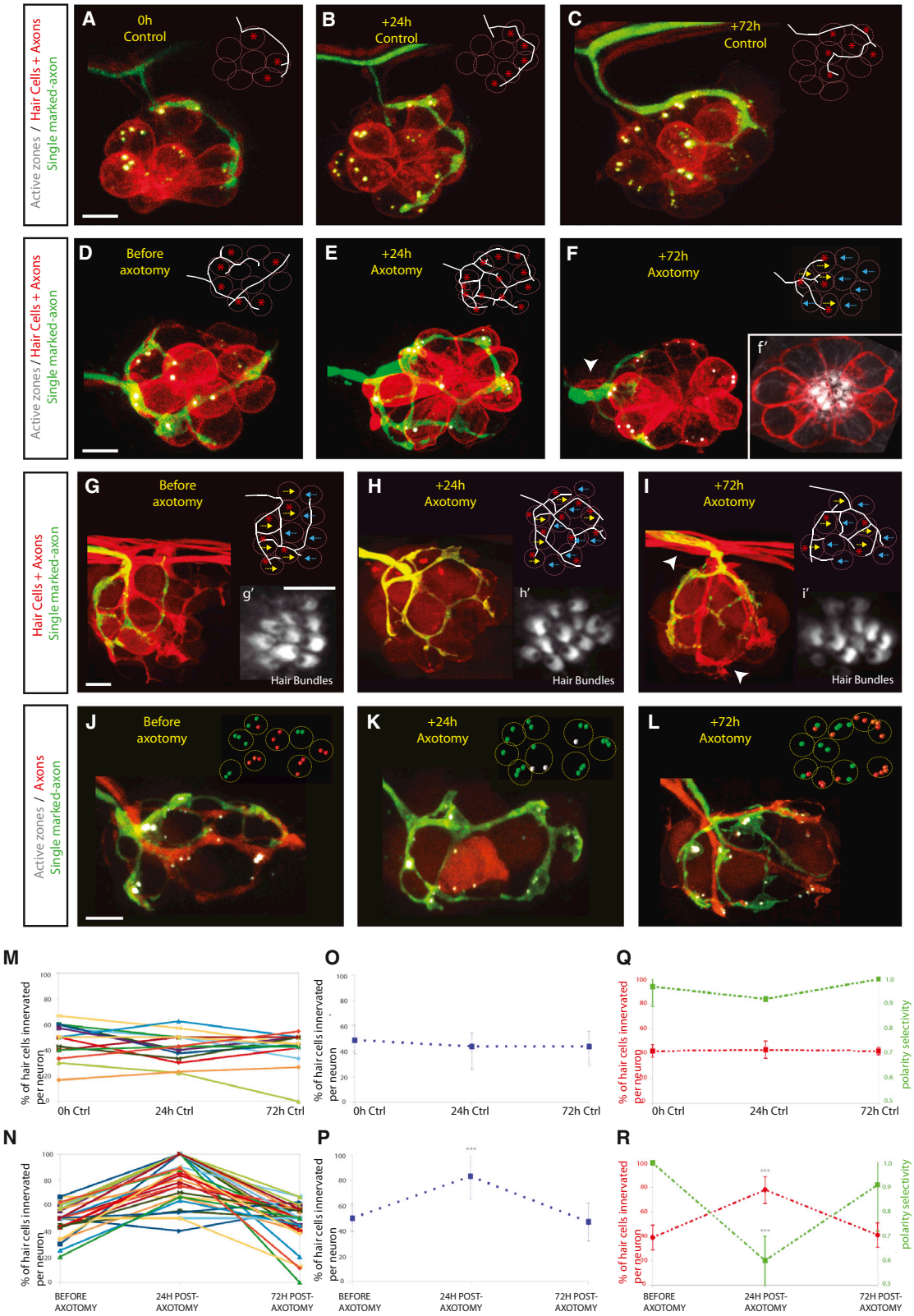

Figure 2. Hair Cell Innervation and Polarity Selectivity in Axotomized Samples

(A–C) 72 hr follow-up of single-marked control axon innervating approximately 50% of hair cells within a neuromast.

(D–F′) Hair cell innervation by single-marked axon in an experimental sample before axotomy (D) and 24 hr (E) and 72 hr (F) after axotomy. The uncut axon (green) synapses every hair cell when solitary (E). Axon regeneration (arrowhead) reverses nonselective innervation (F). Actin labeling with fluorescent phalloidin (F′) reveals hair cell planar polarity in (F).

(legend continued on next page)

using mosaic labeling of neurons and Ctbp2/Ribeye puncta as more accurate markers of synaptogenesis. This experiment confirmed that loss of mechanoreception significantly enhances axonal complexity (Figures S2A–S2E), but it does not affect synaptic selectivity (Table S1). Collectively, these results do not support a model in which polarity-selective synaptogenesis is instructed by evoked mechanosensory activity, and they show that axons cannot autonomously detect the planar polarization of hair cells to exclusively innervate those of a single orientation.

To examine whether this nonselective connectivity by solitary axons can occur postembryonically, we generated solitary axons after the primary lateral line had formed using nitroreductase and the prodrug metronidazole, whose combination produces a toxin that quickly kills nitroreductase-expressing cells [15]. Applying metronidazole to 4 dpf *Tg[SILL1;Brn3c:memEGFP]* double-transgenic larvae with sparse expression of EGFP-nitroreductase resulted in solitary axons that also innervated the majority of the hair cells in NMs at 5 dpf (90% ± 8%, N = 6 NMs) (Figures 1J, 1K, and S1C–S1E). Thus, initially selective axons can become promiscuous upon postembryonic elimination of other converging axons. To further investigate this synaptic plasticity, we took advantage of the regenerative capacity of lateralis peripheral axons after transection [16]. We developed a sensitive protocol for selective axotomy at micrometer resolution by using an ultraviolet laser microbeam, which involves sparse expression of SILL:mCherry to identify a single lateralis afferent neuron in *Tg[Brn3c:Kus-Rib;HGn39D;Brn3c:memEGFP]* triple transgenics, and then severing every EGFP-marked axon, leaving a solitary mCherry-marked axon (Figure S1F). Next, we imaged NMs before axotomy (0 hr) and after axotomy (24 hr and 72 hr). In control (nonaxotomized) fish, each mCherry-marked axon innervated 49% ± 12% of hair cells at 0 hr (N = 20 NMs), 44% ± 11% of hair cells at 24 hr (N = 20 NMs), and 44% ± 11% of hair cells at 72 hr (N = 20 NMs) (Figures 2A–2C, 2M, and 2O). In the experimental fish, before axotomy, each mCherry(+) axon innervated 50% ± 11% of hair cells (N = 37 NMs) (Figures 2D, 2N, and 2P). However, 24 hr after axotomy, each solitary mCherry-marked axon had taken over the presynaptic field and innervated 83% ± 18% of the hair cells (N = 37 NMs) (Figures 2E, 2N, and 2P). Because hair cell turnover is negligible during this period, these solitary axons must have innervated preexisting hair cells of the opposite planar orientation. We also performed the axotomy experiment in *Tg[Myo6b:β-actin-GFP]* transgenic larvae expressing β-actin-GFP in hair cell stereocilia to visualize hair cell planar polarity while observing dynamic connectivity in vivo [17] (Figures 2G–2I). This experiment confirmed that 24 hr after axotomy, solitary axons innervated hair cells of both orientations (N = 11 NMs) (Figures 2H, 2Q, and 2R; Table S2). Remarkably, de novo NM innervation by regenerated EGFP-marked axons 72 hr postaxotomy (Figures 2F, 2I, and 2L) coincided with the reversal of the once-solitary (nonselective) axon transitioning to now synapse with only 47% ± 15% of hair cells (N = 37 NMs) (Figures 2F and 2P), all of which had identical planar polarity (N = 11 NMs) (Figures 2I and 2R; Table S2).

To explore how solitary axons simultaneously innervate hair cells of both planar polarities, we performed dynamic morphometry of individualized axons by measuring the presence, stability, persistence, and consistency of axonal termini. This analysis showed no significant differences between control and solitary axons (Figures S2F–S2N), suggesting that promiscuous innervation is likely due to nonselective stabilization of normal exploratory contacts of solitary axons with denervated hair cells rather than to abnormally enhanced neuritogenesis in the solitary axon. These findings are consistent with persistent postembryonic plasticity in afferent neurons that leads to nonselective innervation in the absence of other axons and with the recovery of selective innervation following the return of other axons to the NM. Importantly, these results are not consistent with repulsion between axons and hair cells of a particular orientation, suggesting that innervation is intrinsically nonselective.

To verify that nonselective innervation by solitary axons represents promiscuous synapses, we immunolabeled membrane-associated guanylyl kinases (MAGUKs) of neuronal postsynaptic densities in *Tg[Brn3c:Kus-Rib;HGn39D;Brn3c:memEGFP]* larvae that had NMs innervated by solitary mCherry(+) axons [11, 18]. Immunohistochemistry showed the juxtaposition, respectively, of presynaptic and postsynaptic densities in hair cells and solitary axonal termini, revealing promiscuous synaptic contacts (N = 4 neurons) (Figures 3A and 3B). However, anatomical connectivity may not result in functional synaptic transmission. Thus, we examined whether mechanical activation of both groups of plane-polarized hair cells would evoke action potentials in the solitary neuron. Because of the opposite arrangement of hair cells within a NM, in normal conditions, bidirectional sinusoid stimuli result in alternating activation of the two populations of hair cells. Consequently, action potentials in a given lateralis neuron only phase lock to one direction of a sinusoidal stimulus [19, 20]. We reasoned that if nonselective synapses were active, solitary neurons should show phase-locked responses to both directions of a sinusoidal stimulus. To test this, we stimulated NMs at 10 Hz while performing cell-attached

(G–I′) Polarity selectivity by single-marked axon in an experimental sample before axotomy (G) and 24 hr (H) and 72 hr (I) after axotomy. The solitary axon (green) innervates hair cells of both polarities (H). Axon regeneration (arrowhead) corrects nonselective innervation (I). β-actin-GFP reveals hair-cell polarity (G′, H′, and I′) in (G), (H), and (I).

Insets in (A)–(F), (G), (H), and (I) quantify synaptic contacts (asterisks). Insets in (F), (G), (H), and (I) also relate hair cell innervation to planar polarity (color-coded arrows).

(J–L) Hair cell innervation by differentially labeled axons in an experimental sample before axotomy (J) and 24 hr (K) and 72 hr (L) after axotomy. Solitary axon (green) innervates every hair cell (K). Reversal to selective innervation coincides with de novo innervation by regenerated axons (red) (L). Insets outline hair cells, showing active zones, color-coded for the type of adjoining axonal termini (green indicates uncut axon, red indicates cut axons, and white indicates no axon).

(M–P) Quantification of hair cell innervation by single-marked axons in control (M and O) and axotomized (N and P) samples from *Tg[Brn3c:Kus-Rib;HGn39D;Brn3c:memEGFP]* animals.

(M and N) Percentage of hair cells innervated by every analyzed axon (color coded).

(O and P) Average of the percentage of hair cells innervated by one axon at the different examined time points.

(Q and R) Quantification of hair cell innervation and polarity selectivity by single-marked axons in control (Q) and axotomized (R) samples from *Tg[Myo6b:β-actin-GFP]* animals. Graphs show the average percentage of hair cells innervated (in red) and average polarity selectivity (in green) by one axon at the different examined time points.

Error bars represent the SD. ***$p < 0.01$ (Student's t test). Scale bars represent 5 μm.

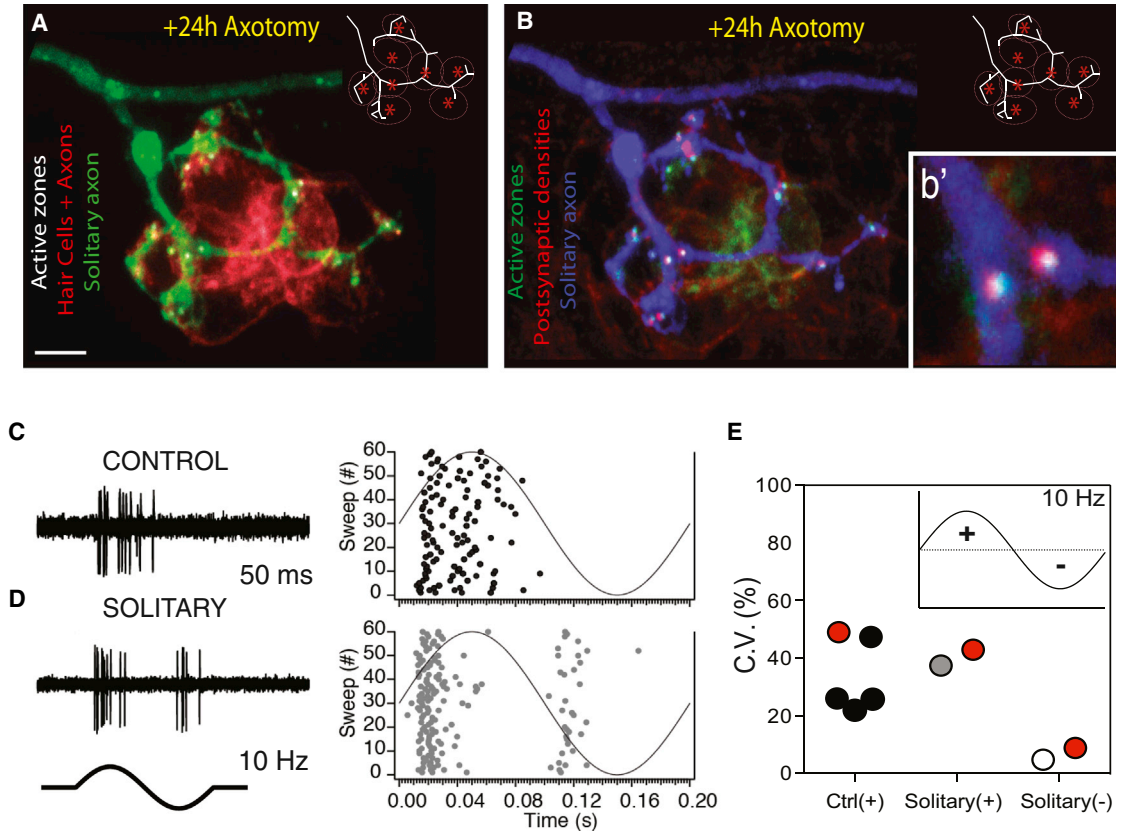

Figure 3. Solitary Axons Form Nonselective Synaptic Connections

(A and B) Synapses between a solitary axon 24 hr after axotomy and all the hair cells within the neuromast (A) revealed by the juxtaposition of presynaptic active zones (Kus-Rib transgene) and postsynaptic densities (pan-MAGUK antibody) (B). Insets quantify synaptic contacts (asterisks). The scale bar represents 5 μm.

(C and D) Electrophysiological recordings from afferent neurons during alternating directional water jet stimulation of the innervated neuromast with 10 Hz sine waves.

(C) A single sweep from a single-marked control neuron that shows phase locking to only one direction of the sinusoid stimulus.

(D) A single sweep from a neuron with a solitary axon after laser ablation of lateralis afferents, showing phase locking to both directions of the sinusoid stimulus.

(E) Coefficient of variation (C.V.) for all the responses during 60 consecutive 10 Hz sweeps for each of the recordings from control neurons, solitary neurons during the positive deflections, and solitary neurons during the negative deflections. Each recording is color coded. The red circles are from the recordings depicted in (C) and (D). The mean C.V. for control experiments is 34% ± 6% (N = 5 neurons), and for solitary neurons the values are 43% and 37%.

extracellular recordings from individual mCherry-marked neurons (Figures 3C–3E and S4; N = 7 neurons). As expected, control neurons displayed phase-locked action potentials in response to only one direction of stimulation (Figures 3C and 3E; N = 5 neurons), whereas solitary neurons displayed phase-locked action potentials to both directions of the stimulus (Figures 3D and 3E; N = 2 neurons). Importantly, all control neurons maintained phase-locked activity to one direction of deflection at frequencies of 10 Hz, 20 Hz, and 40 Hz, whereas the solitary neurons continued to display responses to both directions (data not shown). Collectively, these results demonstrate that solitary axons produce simultaneous functional synapses with hair cells of both planar polarities.

The above findings suggest that synaptic selectivity must emerge from a collective action of the converging axonal population. This scenario is reminiscent of interaxonal competitive processes [21, 22]. Prototypic competitions pit axons against each other, leading to interaxonal avoidance during arbor expansion or to the emergence of winning axons that acquire more synaptic targets [23, 24]. One type of axonal competition underlies synaptic refinement in neuromuscular junctions and sympathetic neurons. By negatively influencing every competing entity (axons or synapses) via limiting access to a resource, competition allows an axon to overcome an intrinsic process that eliminates synapses (other axons would then disengage) or to promote the active elimination of axons (that in the absence of competition would remain engaged). Another form of competition is based on the concept of "synaptic cartels," where an axon innervating a particular "set" of synapses is pitted against the synaptic set of another axon on the same cell [25–27]. The axons forming the outcompeted set eventually disengage together. Importantly, in both cases, axonal competition underlies quantitative aspects of connectivity. One crucial observation in the lateral line is that most axonal arbors are equally complex (Figure S2N) and that winning or losing axons rarely occurs (Figures S2K–S2M), suggesting that lateralis axonal interactions do not meet the above criteria for competition. Another hallmark of competition is the interaxonal exclusion from individual targets. Thus, we asked whether axons exclude one another from individual hair cells by imaging synapses in *Tg[hspGFF53A;UAS:EGFP;SILL1;Brn3c:Kus-Rib]* quadruple transgenics, in

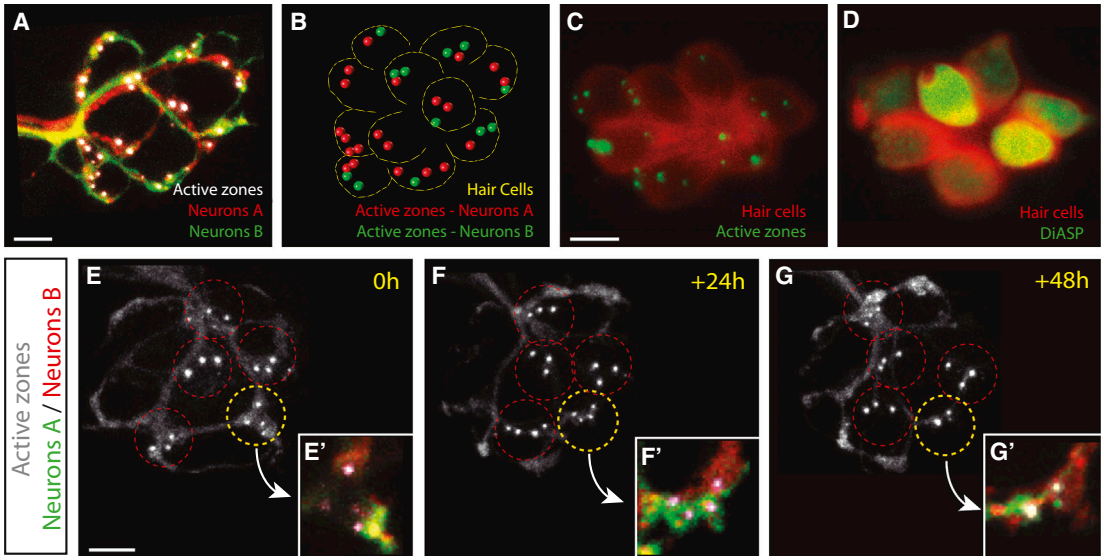

Figure 4. Hair Cell Polyinnervation

(A) Hair cell innervation by differentially labeled axons (revealed by hspGFF53A, in green, and SILL1, in red) in a control neuromast. Hair cell presynaptic active zones are revealed by Rib-Kus transgene.

(B) The dotted circles outline each hair cell in the neuromast shown in (A); the presynaptic active zones are color coded for the type of axonal terminal. 8 out 11 hair cells are polyinnervated.

(C and D) Presynaptic active zones (revealed by Kus-Rib transgene in C) are present in mature hair cells (revealed by DiASP incorporation in D).

(E–G′) Presynaptic active zones in an identified hair cell (yellow outline) are associated to axonal termini from different axons over time.

Scale bars represent 5 μm.

which the spatiotemporal differences in the expression of hspGFF53A (EGFP) and SILL1 (mCherry) individualize axons (Figure 4A). This experiment showed that 60% of the hair cells in NMs simultaneously synapse with two neurons in normal conditions (N = 11 NMs) (Figures 4B–4D). A prospective follow-up of individually identified neurons and hair cells after 48 hr revealed that these polyinnervations were stable (N = 6 hair cells) (Figures 4E–4G), indicating that lateralis axons neither avoid each other nor exclude one another from individual presynaptic targets. Altogether, our results indicate that the interaxonal interactions governing polarity-selective connectivity in the lateral line may be based on a constrained or balanced competition and are more akin to a facilitative process.

Collective axonal interactions may have originated from a primordial process in which axonal populations established and maintained patterns of innervation in a dynamic manner [3, 24, 28]. However, our results demonstrate several fundamental elements that distinguish sensory-neural wiring in the lateral line. First, we rarely observed any loss of axons or axon terminals. Second, we found no axonal exclusion from individual hair cells. Third, interaxonal interactions in the sensory lateral line control a qualitative aspect of connectivity, presynaptic target identity, irrespectively of their number or spatial distribution. Fourth, the interaxonal interaction that we reveal here is postsynaptic because the hair cells represent the presynapse. Fifth, polarity-selective connectivity remains plastic and recurrent after development. We propose that the uncommon combination of the above elements may be a basis of the long-sought mechanism that simultaneously enables the rapid innervation of new receptor cells that arise from the intrinsic repair process of sensory organs, while preserving coherent connectivity patterns. The absence of interaxonal exclusion from individual targets is puzzling and begs the question of what prevents axons from innervating every hair cell in a NM. Because loss of mechanoreception does not alter selectivity, an alternative scenario is that molecular differences between hair cells of each planar-polarity group and complementary chemical labels in neurons prevent axons from innervating every hair cell in NMs. However, no molecular asymmetries between hair cells of either orientation are known, and, importantly, we demonstrate here that putative molecular codes cannot override the indiscriminate innervation by solitary axons. These results led us to conclude that sensory-neural synaptogenesis in the lateral line is intrinsically nonselective. Nevertheless, molecular or activity codes may play a nondeterministic auxiliary role during selectivity. Moreover, codes do not need to be specific to a neuronal or hair cell class to have a powerful influence on selectivity: solely differentiating coherent versus incoherent patterns of innervation would suffice to inform neurons about matched (with a single receptor cell class) versus mismatched synapses. Interestingly, a mutually inhibiting interaction among neurons in *Drosophila* underlies the stereotyped choice of postsynaptic targets in a nondeterministic neural circuit [29]. Thus, the process of selectivity that we show here may be widely employed to control axon-target choices in various regions of the nervous system [30]. Furthermore, a combination of persistent plasticity and selective synaptogenesis independent of predetermination mechanisms has important evolutionary implications because it may provide flexibility for sensory circuits to easily adapt to architectural reorganizations of peripheral organs. For example, retractions, expansions, and/or polarity reorientations of the sensory epithelium would have minimal impact on innervation patterns.

In conclusion, by studying synaptic selectivity in a plane-polarized mechanosensory organ with continuous receptor cell turnover, we found that solitary afferent axons can locate

and innervate a single NM independently of other axons. However, within individual NMs, isolated axons cannot discriminate polarity-selective synapses from nonselective synapses. We propose that interactions among converging postsynaptic axons are essential for the constant recognition of the planar polarization of presynaptic hair cells. Individually, axons may simultaneously innervate hair cells of both polarities by default, but within the context of the converging axonal population, promiscuous synaptogenesis may be less stable. This would suggest that stability and selectivity are mutually dependent. Given that cellular turnover is a widespread strategy to counteract the unavoidable and lifelong environmental damage to sensory organs, this mechanism may represent a common solution to the homeostasis of sensory synaptic selectivity across vertebrates.

Supplemental Information

Supplemental Information includes Supplemental Experimental Procedures, four figures, two tables, and two movies and can be found with this article online at http://dx.doi.org/10.1016/j.cub.2014.11.012.

Author Contributions

J.P.-M. performed intravital imaging, conducted immunohistochemistry, and carried out the axon-cutting experiments together with J.C. A.F. carried out the initial imaging experiments and generated transgenic lines. R.A.-B. and J.G.T. performed electrophysiological recordings. A.A. performed calcium imaging. H.L.-S. assisted in characterizing the transgenic lines. J.P.-M., A.F., J.G.T., and H.L.-S. analyzed and interpreted the data. J.P.-M. and H.L.-S. wrote the manuscript, with input from all the authors.

Acknowledgments

We thank C. Desplan and R. Benton for constructive critique of the manuscript; I. Burtscher and H. Lickert for access to microscopes; the PRBB animal facility, C. Minguillón, and E. Martín-Blanco for zebrafish care. This research was supported by a European Research Council Starting Grant (SENSORINEURAL) and a Programme Grant of the Human Frontier Science Program (RGP0033/2014) to H.L.-S. A.F. was supported by a Marie Curie Fellowship.

Received: July 10, 2014
Revised: September 19, 2014
Accepted: November 5, 2014
Published: December 4, 2014

References

1. Adrian, E.D. (1928). The Basis of Sensation (New York: W.W. Norton & Co.).
2. Hudspeth, A.J. (1989). How the ear's works work. Nature *341*, 397–404.
3. Kaas, J.H. (1989). The evolution of complex sensory systems in mammals. J. Exp. Biol. *146*, 165–176.
4. Ramón y Cajal, S. (1914). Estudios sobre la degeneración y regeneración del sistema nervioso (Madrid: Hijos de Nicolás Moza).
5. Ciba Foundation Symposium 160 (1991). In Regeneration of Vertebrate Sensory Receptor Cells, G.R. Bock and J. Whelan, eds. (Chichester: John Wiley & Sons).
6. Goodman, C.S., and Shatz, C.J. (1993). Developmental mechanisms that generate precise patterns of neuronal connectivity. Cell Suppl. *72*, 77–98.
7. Ghysen, A., and Dambly-Chaudière, C. (2007). The lateral line microcosmos. Genes Dev. *21*, 2118–2130.
8. Faucherre, A., Pujol-Martí, J., Kawakami, K., and López-Schier, H. (2009). Afferent neurons of the zebrafish lateral line are strict selectors of hair-cell orientation. PLoS ONE *4*, e4477.
9. Nagiel, A., Andor-Ardó, D., and Hudspeth, A.J. (2008). Specificity of afferent synapses onto plane-polarized hair cells in the posterior lateral line of the zebrafish. J. Neurosci. *28*, 8442–8453.
10. Schmitz, F., Königstorfer, A., and Südhof, T.C. (2000). RIBEYE, a component of synaptic ribbons: a protein's journey through evolution provides insight into synaptic ribbon function. Neuron *28*, 857–872.
11. Sheets, L., Trapani, J.G., Mo, W., Obholzer, N., and Nicolson, T. (2011). Ribeye is required for presynaptic Ca(V)1.3a channel localization and afferent innervation of sensory hair cells. Development *138*, 1309–1319.
12. Pujol-Martí, J., Zecca, A., Baudoin, J.P., Faucherre, A., Asakawa, K., Kawakami, K., and López-Schier, H. (2012). Neuronal birth order identifies a dimorphic sensorineural map. J. Neurosci. *32*, 2976–2987.
13. Andermann, P., Ungos, J., and Raible, D.W. (2002). Neurogenin1 defines zebrafish cranial sensory ganglia precursors. Dev. Biol. *251*, 45–58.
14. López-Schier, H., and Hudspeth, A.J. (2005). Supernumerary neuromasts in the posterior lateral line of zebrafish lacking peripheral glia. Proc. Natl. Acad. Sci. USA *102*, 1496–1501.
15. Pisharath, H., Rhee, J.M., Swanson, M.A., Leach, S.D., and Parsons, M.J. (2007). Targeted ablation of beta cells in the embryonic zebrafish pancreas using E. coli nitroreductase. Mech. Dev. *124*, 218–229.
16. Villegas, R., Martin, S.M., O'Donnell, K.C., Carrillo, S.A., Sagasti, A., and Allende, M.L. (2012). Dynamics of degeneration and regeneration in developing zebrafish peripheral axons reveals a requirement for extrinsic cell types. Neural Dev. *7*, 19.
17. Kindt, K.S., Finch, G., and Nicolson, T. (2012). Kinocilia mediate mechanosensitivity in developing zebrafish hair cells. Dev. Cell *23*, 329–341.
18. Fuchs, P.A., Glowatzki, E., and Moser, T. (2003). The afferent synapse of cochlear hair cells. Curr. Opin. Neurobiol. *13*, 452–458.
19. Liao, J.C. (2010). Organization and physiology of posterior lateral line afferent neurons in larval zebrafish. Biol. Lett. *6*, 402–405.
20. Trapani, J.G., and Nicolson, T. (2010). Physiological recordings from zebrafish lateral-line hair cells and afferent neurons. Methods Cell Biol. *100*, 219–231.
21. Changeux, J.P., and Danchin, A. (1976). Selective stabilisation of developing synapses as a mechanism for the specification of neuronal networks. Nature *264*, 705–712.
22. Purves, D., and Lichtman, J.W. (1980). Elimination of synapses in the developing nervous system. Science *210*, 153–157.
23. Deppmann, C.D., Mihalas, S., Sharma, N., Lonze, B.E., Niebur, E., and Ginty, D.D. (2008). A model for neuronal competition during development. Science *320*, 369–373.
24. Luo, L., and Flanagan, J.G. (2007). Development of continuous and discrete neural maps. Neuron *56*, 284–300.
25. Colman, H., and Lichtman, J.W. (1992). 'Cartellian' competition at the neuromuscular junction. Trends Neurosci. *15*, 197–199.
26. Loeb, G.E. (1992). Cartels, competition and activity-dependent synapse elimination. Trends Neurosci. *15*, 389–390, author reply 390–391.
27. Ribchester, R.R. (1992). Cartels, competition and activity-dependent synapse elimination. Trends Neurosci. *15*, 389–390, author reply 390–391.
28. Mizumoto, K., and Shen, K. (2013). Interaxonal interaction defines tiled presynaptic innervation in C. elegans. Neuron *77*, 655–666.
29. Langen, M., Koch, M., Yan, J., De Geest, N., Erfurth, M.L., Pfeiffer, B.D., Schmucker, D., Moreau, Y., and Hassan, B.A. (2013). Mutual inhibition among postmitotic neurons regulates robustness of brain wiring in Drosophila. Elife *2*, e00337.
30. Friedrich, R.W., Jacobson, G.A., and Zhu, P. (2010). Circuit neuroscience in zebrafish. Curr. Biol. *20*, R371–R381.